



HAL
open science

Towards brittle materials with tailored fracture properties: the decisive influence of the material disorder and its microstructure

Mathias Lebihain

► **To cite this version:**

Mathias Lebihain. Towards brittle materials with tailored fracture properties: the decisive influence of the material disorder and its microstructure. *International Journal of Fracture*, 2021, *Mathematical and Physical Aspects of Fracture*, 230 (1-2), pp.99-114. 10.1007/s10704-021-00538-7 . hal-03822232

HAL Id: hal-03822232

<https://enpc.hal.science/hal-03822232v1>

Submitted on 20 Oct 2022

HAL is a multi-disciplinary open access archive for the deposit and dissemination of scientific research documents, whether they are published or not. The documents may come from teaching and research institutions in France or abroad, or from public or private research centers.

L'archive ouverte pluridisciplinaire **HAL**, est destinée au dépôt et à la diffusion de documents scientifiques de niveau recherche, publiés ou non, émanant des établissements d'enseignement et de recherche français ou étrangers, des laboratoires publics ou privés.

Towards brittle materials with tailored fracture properties

the decisive influence of the material disorder and its microstructure

Mathias Lebihain

Received: 24 July 2020 / Accepted: 8 April 2021

Abstract Considering a semi-infinite crack propagating within a plane where the local fracture energy fluctuates due to the presence of microstructural heterogeneities, we emphasize the decisive influence of the material disorder on the effective fracture energy of the composite at a macroscopic scale. Through the use of large-scale numerical simulations of a crack interacting with tough inclusions of varying shape, we show how the disorder intensity and the inclusion geometry modify both quantitatively and qualitatively the toughening behavior with respect to the periodic case, where the inclusions are arranged in an ordered manner. This disorder-induced toughening is then rationalized using a theoretical homogenization framework borrowed from statistical physics. It ultimately allows to propose strategies for the design of disordered composites with improved crack growth resistance and tailored asymmetric fracture properties.

Keywords Brittle fracture · homogenization · effective fracture energy · disordered materials · microstructural design

1 Introduction

For a long time, engineers focused on preventing the appearance of cracks in anthropogenic structures. Yet progresses in monitoring techniques showed that cracks were somewhat bound to nucleate in highly loaded components, concentrating thus a lot of attention on the question of their propagation. Based on the pioneering

works of Griffith (1921) and Irwin (1957), the Linear Elastic Fracture Mechanics (LEFM) framework allows nowadays for the quantitative description of the conditions under which preexisting cracks propagate in a homogeneous material. However, our understanding of the impact of microstructural heterogeneities on the overall resistance to crack growth is still largely incomplete. The recent progress in additive manufacturing coupled to the emergence of natural and recycled composite materials further increase the need for rationalizing the failure properties of heterogeneous solids (Merta and Tschegg, 2013; Dimas et al., 2013; Malik and Barthelat, 2016; Chandler et al., 2016; Lei et al., 2018).

Recently, renewed attention has been paid to the quantitative study of the fracture behavior of heterogeneous materials (Barthelat and Rabiei, 2011; Patinet et al., 2013b; Hossain et al., 2014; Xia et al., 2015; Vasoia et al., 2016; Wang and Xia, 2017; Brach et al., 2019; Malik and Barthelat, 2018; Lebihain et al., 2020), in the direct continuation of the pioneering works of (Faber and Evans, 1983), (Gao and Rice, 1989) and (Bower and Ortiz, 1991). These studies provide a detailed description of the impact of small scale microstructural features of materials on their failure at a macroscopic level, in the spirit of the homogenization methods dedicated to elastic and non-linear mechanical properties (Ponte-Castañeda and Suquet, 1997; Milton, 2002). Yet, they are generally restricted to a two-dimensional or periodic setting so they miss major features of the failure behavior, e.g. the intermittent dynamics of cracks (Bonamy and Bouchaud, 2011; Barés et al., 2014) or the scale-invariant roughness of fracture surfaces (Bouchaud et al., 1990; Ponson et al., 2006). In addition, they do not capture the collective pinning involved in brittle solids with randomly distributed tough inclusions, which gives rise to a disorder-induced toughening. Roux

Mathias Lebihain
Laboratoire Navier (ENPC, CNRS UMR 8205, Université Gustave Eiffel),
6-8 avenue Blaise Pascal, 77455 Marne-la-Vallée, France
E-mail: mathias.lebihain@enpc.fr

et al. (2003), Roux and Hild (2008) and Patinet et al. (2013b) rationalized, through a semi-analytical self-consistent approach, the crucial influence of disorder on material toughening. Démary et al. (2014b) addressed the same problem with tools borrowed from statistical physics (Larkin and Ovchinnikov, 1979) to develop a theoretical framework, which allows for analytical predictions of the homogenized fracture properties from the disorder intensity as well as its geometrical structure (Démary et al., 2014a). If these works provide decisive tools to predict the failure behavior of disordered solids, they only consider stochastic distributions of fracture energy that may not be representative of realistic microstructures, and thus make harder the practical design of optimized composites.

The present study aims at filling this gap by investigating the effective fracture energy of micro-structured composites constituted of a homogeneous matrix and tough inclusions with controlled shape and fracture properties. Recently, Lebihain et al. (2021) proposed a homogenization framework that encompasses the influence of both the material disorder and the crack-inclusion mechanisms of interaction localized at the crack tip. They showed that the impact on the effective fracture energy of complex three-dimensional mechanisms could be assessed through the use of equivalent coplanar heterogeneities of fracture energy that are reminiscent from the way the crack interact with the inclusions. We thus consider here the most simple case of a coplanar crack interacting with tough defects, and investigate how the fracture energy and the shape of the inclusions influence the effective fracture properties of the composite in presence of disorder. It allows us (i) to emphasize the major impact of randomness by comparing the disorder-induced toughening with the one resulting from ordered arrangements of heterogeneities, and (ii) to propose strategies to design composites with unique fracture properties, building on the theoretical framework of Démary et al. (2014b).

The paper is organized as follows : in Section 2, we recall the main ingredients behind the perturbative LEFM approach that allows for large-scale simulations of coplanar crack propagation in brittle materials with spatial heterogeneities of fracture energy. Its numerical implementation permits us to investigate in Section 3 the effective fracture energy of composites with circular inclusions in both an ordered and disordered setting. The numerical results are then compared to the theoretical predictions of Gao and Rice (1989) for the ordered case, and Démary et al. (2014b) for the disordered one. Section 4 focuses on the decisive influence of material disorder on the effective fracture energy. Considering several inclusion shapes, we highlight specific situations

where periodic estimates produce neither quantitative nor qualitative predictions on the overall toughening. We finally build on the physics of fracture in disordered media to design composites with asymmetric properties in Section 5, overcoming the smoothing influence of disorder.

2 Coplanar crack propagation in heterogeneous brittle material under pure Mode I loading

Material disorder has been shown to be determinant, alongside the crack-inclusion mechanisms of interaction, to estimate the effective fracture properties of composites. This study aims to shed light on the disorder-induced toughening of composites. We consider then the “simple” case where a coplanar crack interacts with weak heterogeneities of fracture energy G_c through the sole crossing mechanism. This system is analogous to fracture experiments of an interfacial crack propagating between two elastic plates (see e.g. Delaplace et al. (1999); Måløy et al. (2006); Dalmas et al. (2009); Patinet et al. (2013a); Chopin et al. (2018)).

Following a standard LEFM approach (Gao and Rice, 1989; Ponson and Bonamy, 2010; Patinet et al., 2013b; Ponson and Pindra, 2017), we model crack propagation from three main ingredients :

1. the definition of a microstructure, which provides, in our specific case, the spatial field $G_c(\mathbf{x})$ of fracture energy experienced by the crack when propagating;
2. some way to compute the elastic energy release rate (ERR) G along the crack front \mathcal{F} , for any crack configuration differing slightly from a planar crack with a straight front;
3. some propagation criteria, reduced here in single kinetic law that links G_c and G to predict the crack front advance.

The following sections describe how each of these ingredients is accounted for, and how they are connected to each other.

2.1 Material microstructure and heterogeneous fracture energy field

We consider a semi-infinite planar crack embedded in an infinite periodic body. We adopt the usual convention of LEFM and thus denote x the direction of crack propagation, y the direction orthogonal to the crack plane, and z the direction parallel to the crack front \mathcal{F} . Also, the period in the z -direction is denoted L_z and the overall propagation distance L_x . At a given time t , the position of the crack front within the crack plane is

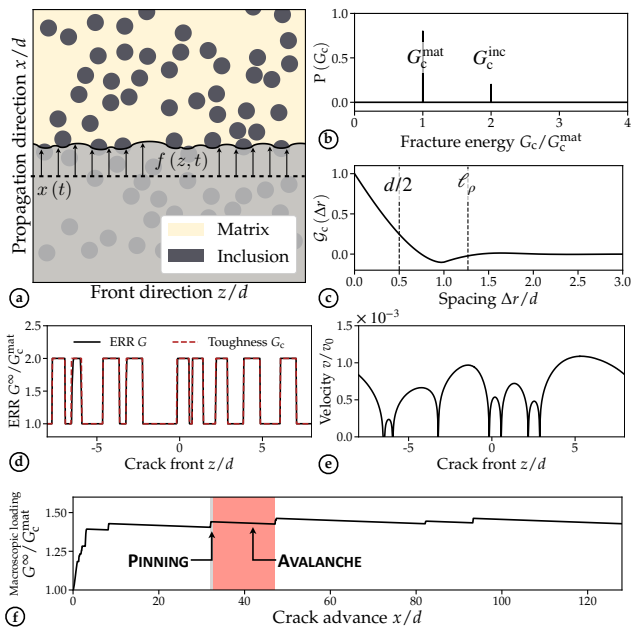


Fig. 1 (a) The coplanar crack front interacts with circular heterogeneities of fracture energy G_c , and distorts in-plane from a straight reference position at $x(t)$ (shifted from the average front position for visualization purpose). (b) The overall distribution of fracture energy is bi-modal, composed of a density ρ_{inc} of inclusions at G_c^{inc} , and one $(1 - \rho_{\text{inc}})$ of matrix material at G_c^{mat} . (c) The spatial texture is described by a correlation function \mathcal{G}_c , characterized by the inclusion diameter d and their average spacing $\ell_\rho \propto d/\sqrt{\rho_{\text{inc}}}$. (d) The front distortions $f(z, t)$ give birth to a heterogeneous local ERR $G(z, t)$ that is compared to the local fracture energy $G_c(z, x = f(z, t))$ to compute (e) the local velocity profile from Eq. (5). (f) The macroscopic loading G_c^∞ from Eq. (1) has to be increased in order to make the crack propagate by successive avalanches separated by pinning phases.

noted $x(t)$, the origin O being chosen arbitrarily within this plane (see Fig. 1.a).

The material is made of two phases: a homogeneous matrix and inclusions of varying geometry. The inclusion distribution is described by its density ρ_{inc} , and the size d_z (resp. d_x) of the inclusion in the crack front (resp. propagation) direction. Two main assumptions are made regarding the mechanical behavior of each phase. First, the matrix and the inclusions are assumed to be isotropically and linearly elastic, and share the same Young's modulus E and Poisson's ratio ν . Second, the phases are assumed to be brittle, i.e. all the dissipative processes located near the crack tip (e.g. plasticity, micro-cracking) are confined in a zone much smaller than the typical heterogeneity size d_z or d_x . However, they differ in their fracture energy: the inclusion fracture energy G_c^{inc} may be larger/smaller than the matrix one G_c^{mat} .

It results in a bi-modal distribution of fracture energy (Fig. 1.b) of average $\langle G_c \rangle$, and standard deviation

σ . The texture $g_c = (G_c - \langle G_c \rangle) / \sigma$ of the material is described by its spatial correlations $\mathcal{G}_c = \langle g_c(r + \Delta r) g_c(r) \rangle_r$, whose decay is characterized by the inclusion radius $d/2$, and their average spacing $\ell_\rho \propto d/\sqrt{\rho_{\text{inc}}}$, defined as the average distance from one inclusion center to that of its nearest neighbor (Fig. 1.c). Note that both the distribution and its texture impact significantly the effective fracture energy of heterogeneous materials (Patinet et al., 2013b; Démary et al., 2014a,b).

The fact that we consider only heterogeneities of fracture energy might appear as a severe limitation of our work. Yet, Lebihain et al. (2021) recently proposed a way to translate richer *intrinsic* mechanisms of interaction (e.g. trapping (Gao and Rice, 1989; Bower and Ortiz, 1991), deflection (He and Hutchinson, 1989; Brach et al., 2019), shielding by micro-cracking (Evans and Faber, 1981; Ortiz, 1987), denucleation/renucleation (Leguillon et al., 2006; Hossain et al., 2014)) into equivalent fracture energy heterogeneities. The equivalent defects of fracture energy can indeed be inferred from the instantaneous front deformations of a semi-infinite crack interacting with a single inclusion, as these distortions are reminiscent of the fracture energy the crack experiences during its propagation (Chopin et al., 2011). The conclusion of our work focused on the disorder-induced toughening may then be applicable to a broader class of heterogeneities.

2.2 Perturbative approach for ERR computation

When considering crack propagation in a heterogeneous material such as the one described in Section 2.1, one must envisage all possible geometric extensions before selecting the path followed during the subsequent propagation event. This specificity provides a natural advantage to perturbative approaches of Linear Elastic Fracture Mechanics. Based on Bueckner-Rice weight function theory (Bueckner, 1970; Rice, 1985), they provide local stress intensity factor variations arising from any small geometrical perturbations of the crack front from a reference crack, without having to solve the whole elasticity problem. Following Gao and Rice (1989), we specialize this approach to the situation investigated in Fig. 1.a.

Macroscopic loading – The semi-infinite crack is embedded in a fracture specimen loaded under tension (Mode I) at a constant opening rate $\dot{\delta}$. The effect of both the loading conditions δ and the sample geometry are included in the proposed model via the evolution of the macroscopic ERR G_c^∞ with the time t and the average crack position $x(t)$. Following Ponson and Bonamy

(2010), G^∞ reads at first-order :

$$G^\infty(t) = G_0^\infty \left(1 + \frac{v_m t - x(t)}{\mathcal{L}} \right) \quad (1)$$

where $G_0^\infty = G^\infty(\delta_0, x=0)$ is the loading for an initial opening δ_0 at $x=0$ and $t=0$. The structural length \mathcal{L} and the driving velocity v_m are defined by:

$$\mathcal{L} = -G_0^\infty / \left. \frac{\partial G^\infty}{\partial x} \right|_{\delta_0,0}; \quad v_m = -\dot{\delta} \left. \frac{\partial G^\infty}{\partial \delta} \right|_{\delta_0,0} / \left. \frac{\partial G^\infty}{\partial x} \right|_{\delta_0,0}. \quad (2)$$

Both \mathcal{L} and v_m are prescribed parameters in the performed simulations. The structural length scale \mathcal{L} is related to the specimen geometry and the loading conditions (usually on the order of one tenth of the specimen length), and controls the evolution of the macroscopic ERR G^∞ as the crack advances. v_m corresponds to the average (in time) crack velocity. An example of the spontaneous evolution of the macroscopic loading $G^\infty(t)$ is shown in Fig. 1.f.

Local energy release rate – In a homogeneous material and under the loading G^∞ , the semi-infinite crack would undergo stable propagation at the speed v_m , and the crack front \mathcal{F} would remain straight at the instantaneous position $x(t) = v_m t$. But the inclusions distort the crack front within the mean fracture plane, giving rise to an in-plane perturbation $f(z, t)$ (see Fig. 1.a), defined from the reference crack position $x(t)$ chosen so as to satisfy the condition $\langle f(z, t) \rangle_z = 0$.

Assuming quasi-static crack propagation¹, one can use the formulæ of Rice (1985) to compute the perturbed ERR G at any position along the crack front. At first order in f , it reads :

$$G(z, t) = G^\infty(t) \left[1 - \frac{f(z, t)}{\mathcal{L}} - \frac{1}{\pi} \text{PV} \int_{-\infty}^{+\infty} \frac{f(z, t) - f(z', t)}{(z - z')^2} dz' \right] \quad (3)$$

We note the presence of long-range elastic interactions along the crack front through the integral terms. This will lead to collective response of the crack during its propagation in a three-dimensional medium as the behavior of a given point along the front is affected by the evolution of all the other ones. An example of the local ERR $G(z, t)$ along a distorted crack front is shown in Fig. 1.d.

¹ The crack speed is assumed to be small with respect to the Rayleigh wave speed at any time and any position along the front. This assumption is generally satisfied even in the presence of the micro-instabilities resulting from the depinning of the crack from tough obstacles, as shown in Chopin et al. (2018).

Equation (3) takes a very simple form when transposed in the Fourier domain :

$$\frac{\hat{G}(k, t)}{G^\infty(t)} = \delta(k) - \left(\frac{1}{\mathcal{L}} + |k| \right) \hat{f}(k, t) \quad (4)$$

where $\hat{\phi}(k, t) = \int_{-\infty}^{+\infty} \phi(z, t) e^{-ikz} dz$ is the z -Fourier transform of a function ϕ and δ is the Dirac function.

Gao and Rice (1989) showed that the perturbative approach of Eq. (3) gives accurate results when compared to boundary elements simulations as long as $G_c^{\text{inc}} \leq 4 G_c^{\text{mat}}$. It sets an upper bound for the inclusion fracture energies considered in this work. This condition also ensures that the crossing mechanism is the only possible mechanism selected by the crack during its interaction with tough inclusions and that no bridging can occur in the crack wake (Bower and Ortiz, 1991).

2.3 Propagation criterion

Given that the motion of the crack is restricted within the plane, the last missing ingredient of our model is the kinetic law that relates the local crack velocity v to G and G_c . For brittle materials, this kinetic law can be derived from Griffith (1921)'s criterion by accounting for the variations of the fracture energy with crack speed (Ponson, 2009; Kolvin et al., 2015). It reads :

$$v = \left[v_m + v_0 \frac{G - G_c(v_m)}{G_c(v_m)} \right]^+ \quad (5)$$

where $[\cdot]^+$ the positive part function, and $v_0 = G_c(v_m) / \left. \frac{\partial G_c}{\partial v} \right|_{v_m}$ is a characteristic velocity of the material that sets the depinning speed at which a crack leaves a tough inclusion. This equation of motion has been shown to capture quantitatively the relaxation dynamics of a crack depinning from a single obstacle (Chopin et al., 2018). An example of the local distribution of velocity $v(z, t)$ is shown in Fig. 1.e.

To satisfy the quasi-static assumption, the driving velocity v_m is set to $v_m = 10^{-9} v_0$ in the remaining of the manuscript.

2.4 Numerical implementation

Random non-overlapping microstructures are built using the so-called random sequential addition algorithm proposed by Widom (1966) that consists in placing randomly and sequentially non-overlapping inclusions on a fixed surface.

The computation of the crack evolution within the heterogeneous fracture energy field $G_c(z, x)$ employs an

explicit scheme that predicts the configuration of the front at time $t + \Delta t$ from its configuration at time t . The crack front is discretized into N points $(P_i)_{i \in [1, N]}$ separated by a uniform distance $\Delta z = L_z/N = d_z/16$, which ensures convergence of the results. First, the ERR G^i is computed by a Fast Fourier Transform (FFT) from the front perturbations f^i using Eq. (4) and from the instantaneous macroscopic loading $G^\infty(t)$ after Eq. (1). It is then compared to the local fracture energy G_c^i to infer the local velocity v^i from the kinetic law of Eq. (5). A stable time step Δt is finally estimated from a Courant-Friedrichs-Lewy condition $\Delta t = 0.1 v_0 \Delta z$, combined with an acceleration procedure based on the physics of depinning (Lebihain, 2019), which is very similar to the one used in the numerical modeling of rate-dependent friction (Lapusta and Rice, 2003). This procedure allows to model the propagation dynamics of a crack interacting with millions of inclusions in only few hours on a single core computer with great accuracy (16 points per inclusion width).

3 Effective fracture energy of heterogeneous materials

The numerical model presented in Section 2 is now used to study the homogenized fracture properties of composite materials. We first clarify what we mean by effective fracture energy in Section 3.1. We then investigate the toughening induced by ordered and disordered arrangements of tough circular inclusions in Section 3.2 and Section 3.3 respectively, highlighting the decisive impact of the material disorder on the ultimate toughening of the composite.

3.1 Homogenized fracture properties and scale-separation conditions

Three possible candidates emerge as potential definitions for the *effective fracture energy* G_c^{eff} (Hossain et al., 2014):

1. The *maximum energy release rate* imposed by the loading during crack propagation G_{max}^∞ (Hossain et al., 2014; Brach et al., 2019; Vasoya et al., 2016), which quantifies the critical loading required to break the whole specimen.
2. The *average energy release rate* imposed by the loading during crack propagation G_{mean}^∞ (Roux et al., 2003; Roux and Hild, 2008; Patinet et al., 2013b), which measure the loading level G_{mean}^∞ at which crack propagation occurs, without necessarily leading to total failure of the structure.

3. the *average dissipation* $\langle G_c^{\text{frac}} \rangle$ defined as the average energy dissipated per unit surface during crack propagation :

$$\langle G_c^{\text{frac}} \rangle = \frac{1}{L_z L_x} \int_{t=0}^{t_{\text{max}}} \int_{z=0}^{L_z} G(z, t) v(z, t) dz dt \quad (6)$$

where $x(t_{\text{max}}) = L_x$. Note that the average dissipation $\langle G_c^{\text{frac}} \rangle$ usually differs from the spatial average of the fracture energy field $\langle G_c \rangle$ due to the micro-instabilities resulting from the depinning of the crack from tough obstacles ($G(z, t) = G_c(v(z, t)) > G_c(v_m)$ in Eq. (5)).

Lebihain et al. (2021) showed that under the scale-separation condition :

$$\mathcal{L} \gg d_z \quad (7)$$

and in the limit of very large systems (Roux et al., 2003; Démercy et al., 2014b), all definitions converge towards a unique value that can be unambiguously defined as the *effective fracture energy* G_c^{eff} of the composite.

In the following, we set $\mathcal{L} = 10^6 d_z$ to satisfy Eq. (7), and measure G_c^{eff} from the peak loading G_{max}^∞ during propagation (see Fig. 2.b).

3.2 Effective fracture energy of periodic media

The notion of effective fracture energy being defined, we now focus on the influence of microstructural parameters, namely the inclusion fracture energy, on the effective fracture energy. We first revisit the case of periodic arrangements of circular inclusions discussed by Gao and Rice (1989) and Bower and Ortiz (1991).

We consider ordered arrangements of circular inclusions of diameter $d = d_z$ at a density $\rho_{\text{inc}} = 20\%$ (see Fig. 3.b), leading to $L_z \simeq 2 d_z$ (see Fig. 2.c). The inclusion fracture energy varies from $G_c^{\text{inc}} = G_c^{\text{mat}}$ to $G_c^{\text{inc}} = 4 G_c^{\text{mat}}$, which remains within the range of validity of the perturbative approach.

The influence of the inclusion fracture energy G_c^{inc} on the effective fracture energy G_c^{eff} is shown in Fig. 2.a. We observe that the effective fracture energy increases linearly with the inclusion fracture energy. Gao and Rice (1989) showed that, for a “regular” penetration process, the effective fracture energy G_c^{eff} reads :

$$G_c^{\text{eff}} = G_c^{\text{mat}} + \frac{d_z}{L_z} (G_c^{\text{inc}} - G_c^{\text{mat}}) \quad (8)$$

which fits the numerical results perfectly (see Fig. 3.a).

The penetration process is said “regular” if it is possible to find a *stable configuration* during crack propagation that satisfy the conditions $G(z) = G_c^{\text{inc}}$ inside the whole inclusion of lateral size d_z , and $G(z) = G_c^{\text{mat}}$ outside of it (Gao and Rice, 1989) (see Fig. 2.c for such a

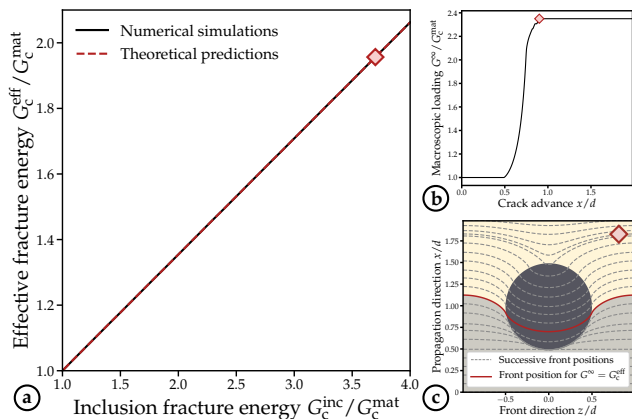


Fig. 2 Effective fracture energy of periodic media with circular inclusions : (a) the effective fracture energy G_c^{eff} (in solid black lines) increases linearly with the inclusion fracture energy G_c^{inc} following Eq. (8) (in dashed red lines). For a given inclusion fracture energy (red square), the effective fracture energy is defined as (b) the maximum macroscopic ERR G_{max}^{∞} imposed during crack propagation. (c) This maximum is reached for a stable crack profile where a portion d_z/L_z of the crack front is crossing the inclusion.

configuration). In such a case, given that $G_c^{\text{eff}} = G_{\text{max}}^{\infty}$ and $G^{\infty} = \langle G(z, t) \rangle_z = \langle G_c \rangle_z$ (see Eq. (4)), we find back Eq. (8). Furthermore, we observe that Eq. (8) only involves a linear density of fracture energy in the direction of the crack front and not in the direction of propagation: the inclusion spacing in the (Ox) direction is then not expected to influence the effective fracture energy in an ordered setting.

In a more general case, Eq. (8) constitutes an upper bound of the effective fracture energy. The regularity of the penetration process is controlled by the inclusion fracture energy, its shape and its density. As we will see in Section 3, it might become “irregular” if the inclusions become tougher, sparser or shorter in the propagation direction (Ox) . The regularity of those penetration processes has been exploited to design orderly arranged composites with asymmetric fracture energy properties (Xia et al., 2013, 2015; Hsueh and Bhattacharya, 2018).

3.3 Effective fracture energy of disordered media

Yet materials are disordered by nature, and despite significant progress in the additive manufacturing techniques, perfectly ordered composites constitute an exception rather than the rule. As it is the case for elastic properties, periodic single-inclusion problems usually allow for a reasonable estimate of the properties of disordered solids as long as a clear separation of scale is valid (Milton, 2002). We can then legitimately wonder if this observation remains valid when homogenizing brittle fracture properties.

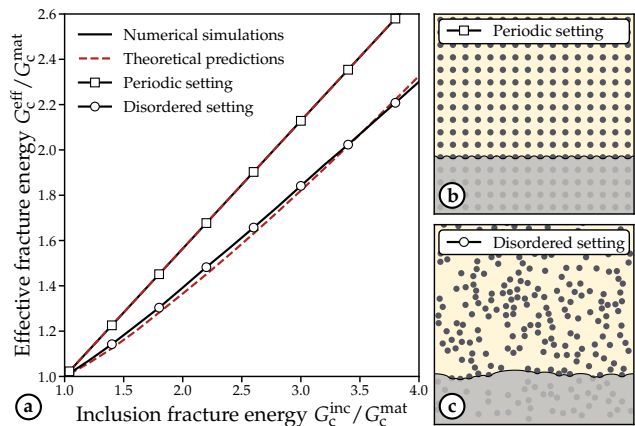


Fig. 3 Effective fracture energy of disordered media with circular inclusions : (a) the effective fracture energy G_c^{eff} differs for (b) periodic and (c) disordered arrangements of circular inclusions, stressing out the major influence of material disorder. Numerical simulations (in solid black lines) are compared to theoretical predictions of equations (8) and (10) (in dashed red lines).

We consider the same situation as before ($\rho_{\text{inc}} = 20\%$ and $1 \leq G_c^{\text{inc}}/G_c^{\text{inc}} \leq 4$), but the circular inclusions are now randomly positioned (see Fig. 3.c²). The system size $L_z = L_x = 256 d_z$ is taken large enough to avoid any influence on the results (Démery et al., 2014b). Variables of interest (front position, macroscopic loading, etc.) are recorded after a propagation length $L_z^* = 16 d_z$ so that a stationary regime independent of the initial planar configuration can be reached (Patinet et al., 2013b). The results plotted in Fig. 3 are averaged over 5 realizations of disorder, i.e. 5 different inclusion distributions, as it will be the case in the remaining of the manuscript.

We observe that the toughening induced by randomly positioned inclusions strongly differs from the one caused by an ordered arrangement. The crossing mechanisms involved during crack growth are indeed radically different: in presence of disorder, the crack dynamics becomes highly intermittent (see Fig. 1.f), and articulate in clusters that span over a broad range of length scales (Bonamy, 2009; Barés et al., 2014). A disorder-induced toughening ultimately arises from the competition between the elasticity of the crack that tends to maintain the front as smooth as possible, and the material disorder that on the contrary tends to roughen it (Démery et al., 2014b).

Démery et al. (2014a) solved the equation of motion of a crack propagating in a stochastic field of fracture

² We show here for visualization purpose $L_z \times L_x = 32 \times 32$ instead of $L_z \times L_x = 256$ as actually performed in our simulations.

energy, which reads at first order :

$$\frac{1}{v_0} \frac{\partial f}{\partial t}(z, t) = \frac{v_m}{v_0} + \frac{G^\infty}{\langle G_c \rangle} - \frac{f(z, t)}{\mathcal{L}} \quad (9)$$

$$- \frac{1}{\pi} \text{PV} \int_{-\infty}^{+\infty} \frac{f(z, t) - f(z', t)}{(z - z')^2} dz' - \frac{\sigma}{\langle G_c \rangle} g_c(z, x = f(z, t))$$

where $\langle G_c \rangle = G_c^{\text{mat}} + \rho_{\text{inc}} (G_c^{\text{inc}} - G_c^{\text{mat}})$ and $\sigma = \sqrt{\rho_{\text{inc}} (1 - \rho_{\text{inc}})} (G_c^{\text{inc}} - G_c^{\text{mat}})$ are the average and the standard deviation of the fracture energy field $G_c(z, x)$, and ξ_z (resp. ξ_x) its correlation length in the front (resp. propagation) direction, which can be approximated in our case as d_z (resp. d_x).

They showed that, when the disorder is weak enough, the crack propagates in a *collective pinning regime* and the effective fracture energy is given by (Démery et al., 2014a):

$$G_c^{\text{eff}} = \langle G_c \rangle + \frac{\sigma^2}{\langle G_c \rangle} \cdot \frac{\xi_z}{\xi_x} \quad (10)$$

The effective fracture energy is governed by the distribution of fracture energy experienced, during pinning phases where the crack front is stuck, by portions of the crack front of size :

$$L_c = \left(\frac{\langle G_c \rangle}{\sigma} \right)^2 \frac{\xi_x^2}{\xi_z} \quad (11)$$

called ‘‘Larkin domains’’ (Larkin and Ovchinnikov, 1979).

An additional toughening $\frac{\sigma^2}{\langle G_c \rangle} \frac{\xi_z}{\xi_x}$ then emerges from the material disorder σ , a feature that had been already observed with the self-consistent approach of Roux et al. (2003) in Patinet et al. (2013b). Roughly speaking, the crack front ends up to get stuck by the toughest inclusions so it effectively visits regions of the local fracture energy field that are tougher than the average value $\langle G_c \rangle$. Note that the material texture $g_c = (G_c - \langle G_c \rangle) / \sigma$ influences the toughening arising from the positional disorder. In particular, oscillations due to exclusion effects (impenetrable inclusions) are likely to increase the disorder-induced toughening (Démery et al., 2014a).

The theoretical predictions of Démery et al. (2014a) happens to be in good agreement with our numerical results as it can be seen in Fig. 3. Several remarks are in order :

- periodic simulations do not provide *quantitative estimate* on the effective fracture energy of disordered materials, as it can be seen from the theoretical formulæ of Eq. 8 for ordered arrangements of inclusions and Eq. 10 for disordered ones;
- the physics underlying both types of toughening is very different by nature. One relies on the regularity of the penetration process at the inclusion scale, while the others involves collective effects at a scale

given by the Larkin length L_c of Eq. (11) that can contain dozens/hundreds of inclusions. One thus expects that periodic simulations may even predict toughening behaviors that are *qualitatively* wrong; in particular, increasing the elongation ratio d_x/d_z of the inclusions has been shown to improve the regularity of the penetration process (Gao and Rice, 1989), while it appears from Eq. (10) to influence negatively the disorder-induced toughening.

These three points are illustrated in the Section 4 to highlight the tremendous impact of material disorder on the effective fracture energy.

3.4 Finite size effects on the effective fracture energy

Before exploring in greater details the influence of material disorder on the effective fracture energy, we first discuss how finite size effects may qualitatively influence the results presented thereafter. Indeed, we measure in this work the effective fracture energy in the special case of a semi-infinite crack embedded into an infinite periodic solid. In real experiments, fracture specimens have a finite (i) length, (ii) height, and (iii) width, that may or may not change our results:

1. finite length effects can be grasped within the structural length scale \mathcal{L} that accounts for the macroscopic ERR G^∞ decrease with crack advance. In an *ordered* setting, a more stable geometry (low \mathcal{L} or small specimens) dampens the front deformations, and thus enforces the regularity of the penetration processes. The maximal loading G_{max}^∞ is not expected to deviate much from G_c^{eff} of Eq. (8), but the average dissipation $\langle G_c^{\text{frac}} \rangle$ may fluctuate between $\langle G_c \rangle$ (for $\mathcal{L} \lesssim d_z, d_x, \ell_\rho$) and G_c^{eff} of Eq. (8) (for $\mathcal{L} \gg d_z, d_x, \ell_\rho$). In a *disordered* setting, the finite length of the system might bring the effective toughness down to the weak pinning limit $G_c^{\text{eff}} = \langle G_c \rangle$ for $\mathcal{L} \lesssim d_z$ (Démery et al., 2014a; Lebihain et al., 2021).
2. finite height effects can be accounted for within the perturbative approach of LEFM building on the results of Legrand et al. (2011) that extended Rice (1985)’s formulæ to the case of a semi-infinite planar crack located in the mid-plane of a thin plate. In the limit case of an infinite thin plate, the non-local contributions of Eq. (3) are enhanced by a factor 4 due to the finite height of the system. Thus, for *ordered* systems, finite height effects smooth out crack front deformations, which enforces again the regularity of the penetration process. The effective fracture energy G_c^{eff} follows then Eq. (8). For *disordered* systems, the amplification of the non-local interactions are expected to decrease the size L_c of

the Larkin domains (Démery et al., 2014b), which leads to an overall toughening of the material. Note that such an effect is not expected to modify *qualitatively* the observations of Sections 4 & 5.

3. finally, to the best of the author's knowledge, the perturbative approach used in this paper cannot account for finite width effects, as the anticlastic deformations of the specimen that lead to a curved crack front (Jumel and Shanahan, 2008-09-22; Patinet et al., 2013a). Yet, when the curvature of the front is larger than the defect spacing (in an ordered case) or the Larkin domains (in a disordered one), one may assume that the effective fracture energy is not influenced much by the finite width of the system.

4 From periodic to disordered microstructures: the major impact of the material disorder

This section aims at stressing out that material disorder *must not be ignored* when designing tougher materials. Playing with the shape of the inclusions, namely their size ratio d_x/d_z , we show that designing composites from periodic simulations can result in *quantitative* errors on the ultimate toughening (Section 4.1), and may even lead to misjudge the toughening behavior of a given geometry (Section 4.2). Based on this results, we finally highlight counterintuitive impacts of the material disorder in Section 4.3.

4.1 Estimating the effective fracture energy of disordered composites from periodic simulations can lead to quantitatively wrong predictions

We consider a situation similar as the one presented in Section 3 where tough circular inclusions, whose fracture energy varies from $G_c^{\text{inc}} = G_c^{\text{mat}}$ to $G_c^{\text{inc}} = 4 G_c^{\text{mat}}$, are randomly distributed with a slightly lower density $\rho_{\text{inc}} = 10\%$. But here, we increase the aspect ratio $r = d_x/d_z$ from $r = 1$ (circle) to $r = 4$ (ellipsoid elongated along the propagation direction) (see Fig. 4), while keeping the ratio d_z/L_z constant for all considered geometries in order to remove the influence of the system size (Démery et al., 2014b). The distribution of elliptical inclusions are generated from a circular one by dilating the inclusion position x and its size d_x by a factor r , so that all the characteristic length scales of the disorder texture (inclusion size d_x and spacing ℓ_ρ^x) evolve accordingly.

In the periodic case, we observe in Fig. 4.a that the inclusion elongation does not impact the effective fracture energy when the elongated inclusion is oriented in the propagation direction, and still follows Eq. 8. It is

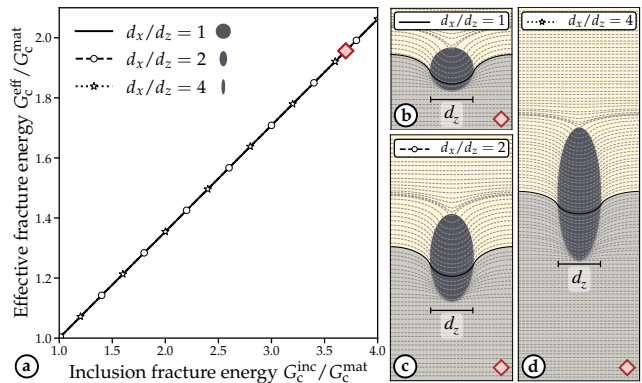


Fig. 4 (a) Effective fracture energy of periodic media with tough inclusions elongated along the propagation direction : all the composites display the same toughening behavior described by Eq. (8) as the inclusion fracture energy is increased since (b-d) the crossing processes are regular for all considered geometries.

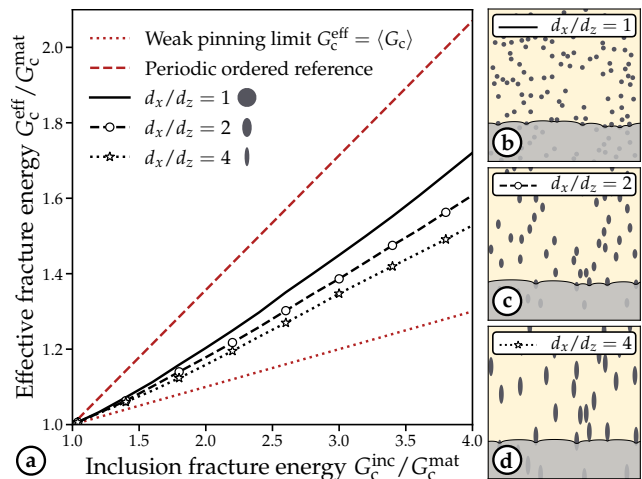


Fig. 5 (a) Effective fracture energy of disordered media with tough inclusions elongated along the propagation direction : the toughening increase driven by material disorder is reduced as (b-d) the inclusion gets more and more elongated along the direction (Ox) of propagation. The periodic ordered case (dashed red lines) and the weak pinning limit $G_c^{\text{eff}} = \langle G_c \rangle$ (dotted red lines) are plotted for reference.

explained by the fact that the inclusion elongation does not influence the regularity of the penetration process, since we can always find a stable configuration where $G(z) = G_c^{\text{inc}}$ on a portion of size d_z of the inclusion and $G(z) = G_c^{\text{mat}}$ outside of it (see Fig. 4.(b-d)).

When disorder is introduced, the toughening behavior differs for the three considered geometries (see Fig. 5). The Larkin domains spread wider (see Eq. (11)) and the disorder-induced toughening is smoothed down toward the *weak pinning* limit $G_c^{\text{eff}} = \langle G_c \rangle$ corresponding to the limit $d_x/d_z \rightarrow \infty$ (Roux et al., 2003). This toughening decrease as the inclusions become longer (increase of d_x/d_z) is well predicted by Eq. (10).

Inclusion geometries, which produce the same toughening in the periodic case, can lead to different toughening behaviors as soon as disorder is introduced. Thus, periodic estimates do not provide *quantitative* predictions on the effective fracture energy of disordered composites.

4.2 Neglecting the impact of material disorder may lead to qualitatively wrong predictions of the effective fracture energy

We now show that periodic estimates can be even *qualitatively* wrong in predicting the influence of the inclusion shape on the toughening behavior of brittle composites, and consider inclusions elongated along the front direction (Oz) with a size ratio d_x/d_z ranging from $d_x/d_z = 0.25$ to $d_x/d_z = 1$.

In the periodic case of Fig. 6, we observe that when the inclusion gets too elongated and tough, the overall toughening decrease from the circular case. For low (Oz)-elongation ratio ($d_x/d_z = 0.5$ or $d_x/d_z = 1$), the penetration process remains regular (see Fig. 6.(b-c)), and the effective fracture energy follows the theoretical predictions of Eq. (8). For larger elongation ratios ($d_x/d_z = 0.25$) and significant fracture energy contrast ($G_c^{\text{inc}} \geq 2.2 G_c^{\text{mat}}$), the penetration process becomes unstable: in Fig. 6.d, we observe that parts of the crack front located on the sides of the inclusion unpin first, reducing the inclusion width at the critical load and the effective fracture energy (see Eq. 8). As the inclusions get tougher, this lateral crossing starts earlier and induces an overall decrease of the composite fracture energy.

When disorder is introduced, the toughening behavior shifts drastically (see Fig. 7): in contrast with the periodic case where high (Oz)-elongation ratios tend to decrease the effective fracture energy, it toughens the material in presence of disorder. It emerges from the contraction of the Larkin domains with decreasing d_x/d_z (see Eq. (11)). The critical loading to make the crack propagate further increases with respect to the *weak pinning* limit $G_c^{\text{eff}} = \langle G_c \rangle$, that corresponds to the absence of disorder. This feature is well grasped by Eq. 10.

An inclusion geometry, which appears to be detrimental to material toughening in a periodic setting, proves to be beneficial in presence of disorder. Thus, periodic estimates may not provide *qualitative* predictions on the toughening behavior of disordered composites.

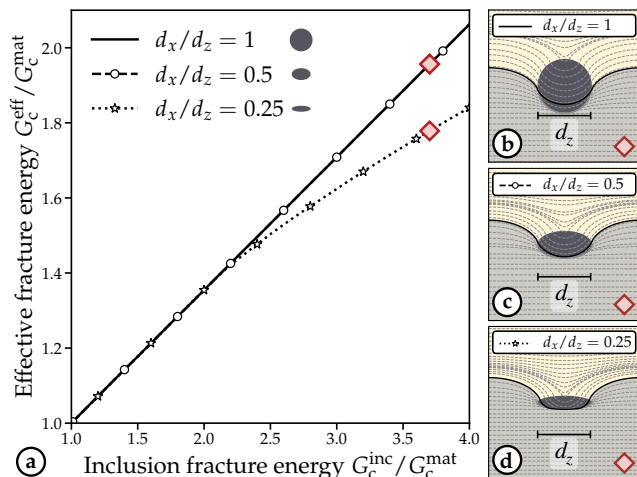


Fig. 6 (a) Effective fracture energy of periodic media with tough inclusions elongated along the front direction : material toughening for low elongation ratio ($d_x/d_z = 1$ and $d_x/d_z = 0.5$) follows Eq. (8) since (b-c) the crossing processes are regular. At higher inclusion elongation ($d_x/d_z = 0.25$), these processes become unstable due to (d) early crossing at the sides of the inclusion, leading to a decreased toughening.

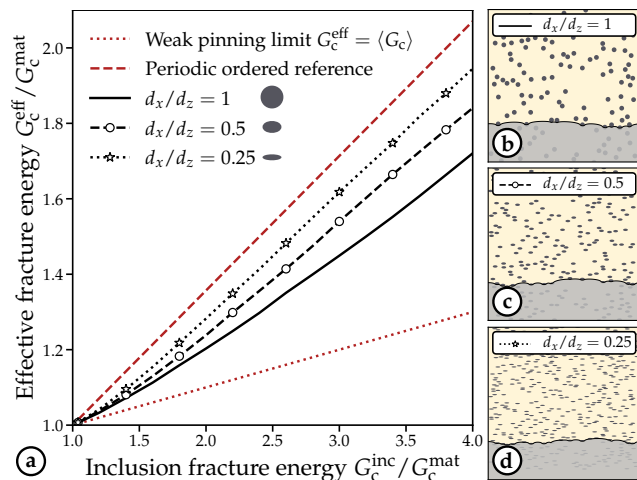


Fig. 7 (a) Effective fracture energy of disordered media with tough inclusions elongated along the front direction : in contrast with the periodic setting of Fig. 6, the disorder-driven toughening increases as (b-d) the inclusion gets more and more elongated along the front direction (Oz). The periodic ordered case for the circle inclusion (dashed red lines) and the weak pinning limit $G_c^{\text{eff}} = \langle G_c \rangle$ (dotted red lines) are plotted for reference.

4.3 Counterintuitive impacts of the material disorder for the design of tougher composites

Now that we understand how the elongation of the inclusions impacts the effective fracture energy in presence of disorder, we highlight some counterintuitive effects that only emerge from the disorder-induced toughening.

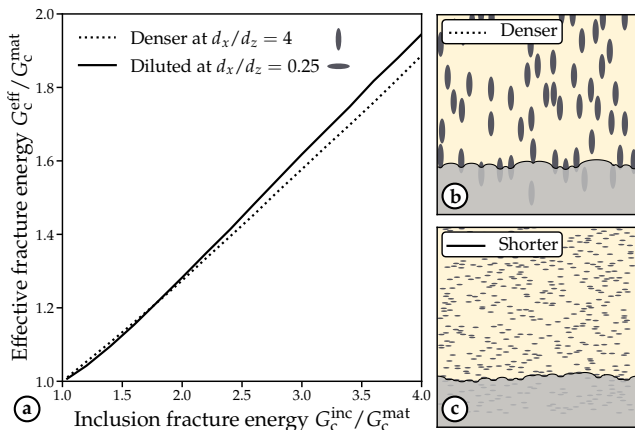


Fig. 8 (a) Influence of the inclusion geometry in tuning material toughening : (b) microstructure with increased density ($\rho_{\text{inc}} = 20\%$ in solid line) can have a lower toughening impact if the inclusions are elongated along the propagation direction ($d_x/d_z = 4$) rather than in the front direction ($\rho_{\text{inc}} = 10\%$ and $d_x/d_z = 0.25$ in dashed line).

Denser yet weaker – First, we show that, at constant inclusion fracture energy, denser distributions of inclusions might not lead to toughening. We consider first a distribution of inclusions elongated along the (Oz)-direction of the crack front ($d_x/d_z = 0.25$) at a density $\rho_{\text{inc}} = 10\%$ and a second distribution of inclusions elongated along the (Ox)-direction of propagation ($d_x/d_z = 4$) at a density $\rho_{\text{inc}} = 20\%$. We observe in Fig. 8 that the second distribution is slightly weaker than the first one despite being *twice denser*. Such an observation is very specific to the disordered setting and does not remain valid in the periodic one.

Weaker yet not weaker – Now we prove that, in presence of disorder, the introduction of weak inclusions does not necessarily weaken the composite. We consider the joined cases of Sections 4.1 and 4.2, but we now allow the inclusions to be slightly weaker than the matrix, with a constant fracture energy ranging from $0.5 G_c^{\text{mat}}$ to $1.5 G_c^{\text{mat}}$. We observe in Fig. 9 that introducing weak patches usually lead to an overall weakening of the composite (for $d_x/d_z = 1$ and $d_x/d_z = 4$), but also that the effective fracture energy remains unchanged when the weak inclusions are elongated along the direction of the crack front ($d_x/d_z = 0.25$). Again, as the inclusions get more and more elongated along the (Oz)-direction of the crack front, the Larkin domains shrink (see Eq. (11)) until they only contain matrix material. The critical loading required to unpin this portion of the crack front is then equal to the fracture energy of the matrix $G_c^{\text{eff}} = G_c^{\text{mat}}$. It is interesting to note that the theoretical formula of Démary et al. (2014a) from Eq. (10) predicts a toughening $G_c^{\text{eff}} > G_c^{\text{mat}}$ in presence of weak inclusions elongated along the front direction.

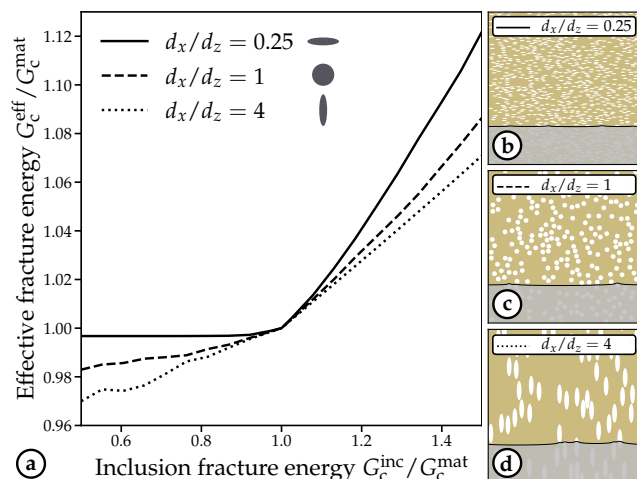


Fig. 9 Influence of the inclusion geometry in suppressing the impact of material defects : the introduction of weaker inclusions usually weakens the composite (b-c) except when the inclusions are elongated along the front direction (d) where the disorder tunes down the influence of weak patches.

It misses the fact that the effective fracture energy *can never be higher than the maximum value of the local fracture energy field*, since it is set by the fracture energy experienced by a Larkin domain.

5 Designing composites with asymmetric fracture energy properties in presence of disorder

Several works took advantage of the regularity of the penetration process that governs material toughening in periodic setting, to design ordered composites with asymmetric fracture properties (see e.g. Xia et al. (2013) Xia et al. (2015), and Hsueh and Bhattacharya (2018)). Since the introduction of disorder can strongly affect the toughening behavior for a given inclusion geometry, we can wonder whether this fracture energy asymmetry survives when the inclusion are positioned at random. We show in Section 5.1 that the peculiar mechanisms of crack propagation in disordered media may smoothen out the geometry-induced asymmetry, but that one can still design proper inclusion shape to achieve asymmetric failure properties as illustrated in Section 5.2.

5.1 Disorder may smoothen out toughening asymmetry

We saw in Section 4.2 that low elongation ratio d_x/d_z can trigger irregular penetration process due to the early crossing of the inclusion sides. We then consider an inclusion, which is made of two semi-ellipses with $d_x/d_z = 0.125$ on top and $d_x/d_z = 0.5$ on the bottom

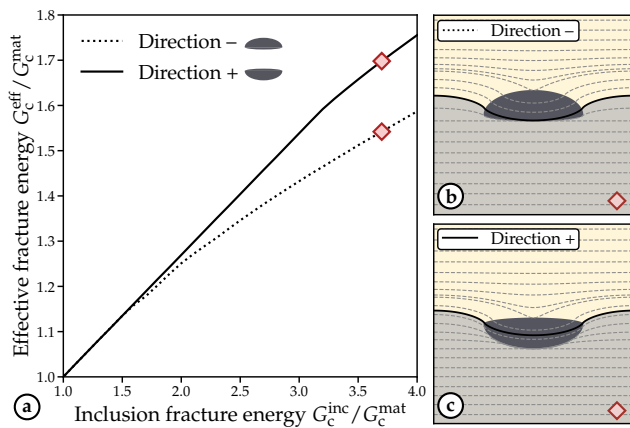


Fig. 10 (a) Fracture energy asymmetry for periodic arrangements of asymmetric inclusions : the inclusion shape render the penetration process (b) regular when the thicker portion is facing the incoming crack and (c) irregular in the other direction, leading to asymmetric toughening.

(see Fig. 10), and study the effective fracture energy of such composites at $\rho_{\text{inc}} = 12\%$.

In a periodic setting, an expected asymmetry of effective fracture energy emerges from the (ir)regularity of the penetration process depending on which part of the inclusion the crack faces first (see Fig. 10): when the crack lands on the thin ellipse, the penetration phase is unstable with early lateral crossing (Fig. 10.b), while it is mostly stable when facing the thicker one (Fig. 10.c). The effective fracture energy asymmetry increases as the inclusion fracture energy gets bigger and the penetration process gets more irregular.

The introduction of disorder tends to smoothen out this fracture energy asymmetry (see Fig. 11). This is explained by the fact that the effective fracture energy of Eq. 10 (and the size of the Larkin domains L_c of Eq. 11) involves the correlation lengths ξ_z and ξ_x of the fracture energy field $G_c(z, x)$, which are invariant with the transformation $x \rightarrow -x$. Thus, the macroscopic fracture energy of the composite is not expected to depend on the orientation of the microscopic inclusions in presence of disorder. The slight anisotropy observed in Fig. 11.a will be discussed in the next section.

5.2 Tuning the inclusion geometry to force fracture energy asymmetry

Even though it is well captured by the framework of Démary et al. (2014b), this smoothening of the geometry-driven fracture energy asymmetry in presence of disorder is detrimental to the design of optimized composites with tailored fracture properties. However, we show in this last section that it is possible to overcome this effect, and design disordered materials with asymmetric

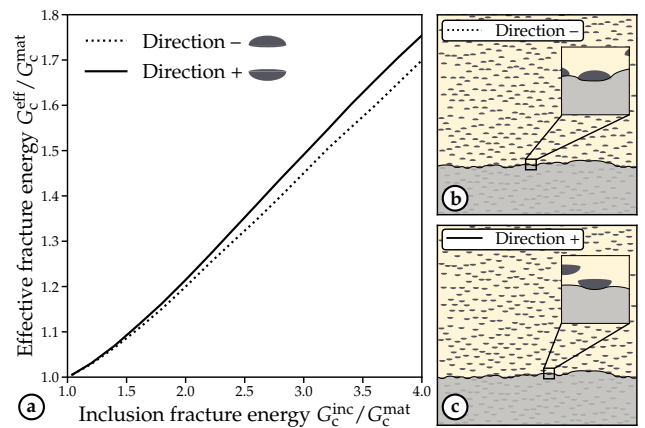


Fig. 11 (a) Fracture energy asymmetry smoothened by disorder for asymmetric inclusions : the asymmetric toughening observed for periodic arrangements in Fig. 10 almost completely disappears in presence of disorder. (b-c) Toughest configurations of the crack front for each inclusion orientation.

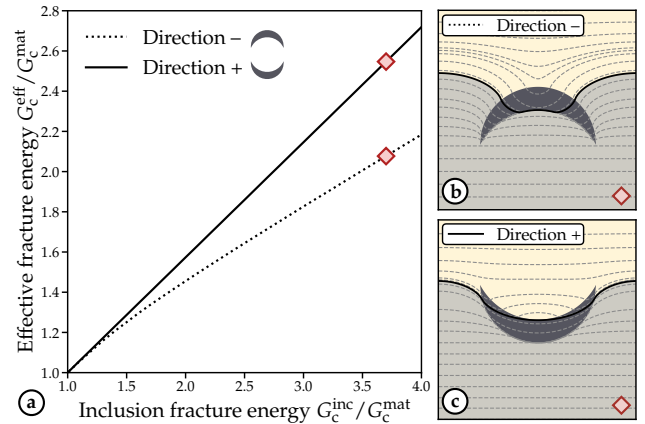


Fig. 12 (a) Fracture energy asymmetry for periodic arrangements of moon-shaped inclusions : the inclusion shape make penetration processes (b) regular when the inclusion tip are away from the incoming crack and (c) irregular in the other direction, leading to an asymmetric toughening.

fracture energy, building on the specific collective crossing mechanisms involved.

We consider now moon-shaped inclusions, inspired by the seminal study of Xia et al. (2013). The presence of peaked parts on both sides of the inclusions trigger strongly irregular penetration processes when the crack front faces those peaks (Fig. 12.b), while the larger curvature in the other direction allows for stable crossing of the inclusion (Fig. 12.c). Consequently, the effective fracture energy displays a strong asymmetry in a periodic setting (see Fig. 12.a), reported in Xia et al. (2013), Xia et al. (2015), and Hsueh and Bhattacharya (2018).

Surprisingly, we observe in Fig. 13.a that this fracture energy asymmetry survives to the presence of disorder, contrary to the case presented in Section 5.1. It is explained by the fact that the effective fracture energy

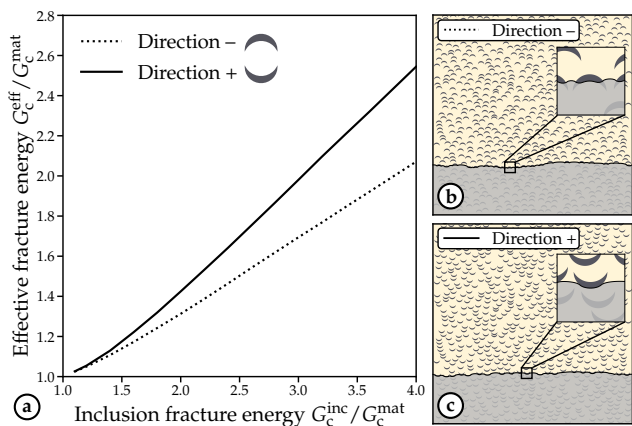


Fig. 13 (a) Fracture energy asymmetry persists in presence of disorder for moon-shaped inclusions : the effective fracture energy is linked to the critical force required to make propagate a Larkin domain from (b-c) a pinning configuration, and thus depends on (insets b-c) the pinning configuration at the inclusion level.

is set by the critical force required to unpin a Larkin domain. The size L_c of a Larkin domain relates to the amplitude of the crack front roughness *in a pinning configuration*³, which might be sensitive to the details of the microstructure. Such a pinning configuration is plotted for both inclusion orientations in Fig. 13.(b-c). We observe (in inset) that the pinning configuration on each inclusion strongly depends on the inclusion orientation, and gives rise to a smaller effective inclusion width d_z^{eff} when the peaks of the moon-shaped inclusion are facing the crack (Fig. 13.b), while its effective length d_x^{eff} remains fairly unchanged. Based on Eq. (10), this tends to reduce the disorder contribution $\frac{\sigma^2}{\langle G_c \rangle} \frac{\xi_z}{\xi_x}$ and thus explains why we can still observe fracture energy asymmetry in presence of disorder. In particular, we see in Fig. 11.(b-c) that, in the case of joined-ellipsoids inclusions, the effective size ratio $d_x^{\text{eff}} / d_z^{\text{eff}}$ is almost independent of the inclusion orientation, giving rise to a quasi-symmetric effective fracture energy.

This last example highlights the importance of accounting for the influence of material disorder when designing tougher materials. Assuming periodicity might be both *quantitatively* and *qualitatively* wrong in estimating the effective fracture energy of realistic composites, in which perfect order is often out of reach. Yet, periodic simulations may constitute an efficient means of estimating the relevant parameters (ξ_z , ξ_x) feeding the theoretical model of Démary et al. (2014b) that accounts for the decisive influence of disorder, as illustrated in the previous example.

³ The Larkin length is defined through the relation $\Delta f(\Delta z = L_c) = \xi_x$, where $\Delta f(\Delta z) = \langle [f(z + \Delta z, x) - f(z, x)]^2 \rangle^{1/2}$ is the correlation function of the in-plane front perturbation.

6 Conclusion

This work highlights the dramatic influence of material disorder on the effective fracture energy of brittle composites. Considering the most “simple” case of a coplanar crack propagating in 3D within a heterogeneous fracture energy field $G_c(z, x)$ arising from realistic microstructures, we study the ultimate toughening resulting from randomly positioned inclusions, and compare it to the one induced by ordered arrangements (corresponding to a single inclusion problem in a periodic setting). We conclude that the effective fracture energy of disordered brittle composites cannot be inferred from periodic simulations. More precisely, various key results can be retained from this work:

- the toughening induced by disordered arrangements of tough inclusions strongly differs from the ordered case. Designing composites from periodic simulations might lead to *quantitative* errors on the ultimate inclusion-induced toughening. It is explained by the fundamentally different mechanisms involved during the pinning/depinning of the crack front by the inclusions: in the ordered case, the regularity of the penetration process is crucial (Gao and Rice, 1989), while in presence of disorder, the effective fracture energy is dictated by the fracture energy experienced during a pinning configuration by a Larkin domain, emerging from the disorder intensity and its geometrical structure;
- the toughening behavior displayed by a given inclusion geometry as its fracture energy increases cannot be inferred from the periodic case, which can be (i) *quantitatively* and (ii) *qualitatively* different. We considered (i) elliptic inclusions elongated along the propagation direction, which toughens the composite equally no matter the elongation ratio when orderly disposed, and differently when positioned at random. The toughening behavior predicted by periodic simulations may then be *quantitatively* wrong. We then investigated (ii) elliptic inclusions elongated along the front direction, and showed that the inclusion-induced toughening was reduced in the periodic case as their elongation was increased, while it increases in presence of disorder. Periodic computations can thus predict a toughening behavior that is *qualitatively* wrong.
- the toughening induced by the material disorder being linked to both the disorder intensity σ and its geometrical structure ξ_z / ξ_x , one can design brittle materials with surprising properties such as one tougher than the other despite having half the density of inclusions of same fracture energy. One can

also design composites that doesn't get weaker as its inclusion phase gets weaker and weaker.

- material design should include the influence of disorder otherwise astonishing properties, such as fracture energy asymmetry, might disappear when the inclusions are positioned at random. A careful design of inclusion geometry that complies with the physics of brittle fracture in heterogeneous media may lead to the development of tough composite with surprising fracture properties.

Regarding the last point, the persistence of a fracture energy asymmetry in a disordered setting is unexpected, since it cannot be grasped by the direct application of the theoretical formulæ of Démary et al. (2014a). The effective fracture energy appears to be strongly dictated by the fracture energy experienced by the front during pinning configurations, and depends then on the details of the microstructure at the inclusion level. Surprisingly, the stable configurations observed in the periodic case could provide some insight on the pinning configuration at the inclusion level in presence of disorder. These preliminary results open a promising route to the careful design of anisotropically tough interfaces.

Despite its limiting assumptions (e.g. coplanar propagation, constant elasticity, weak disorder), our results give useful insights on the sole influence of material disorder and its microstructure on the effective fracture energy. Bearing in mind that more complex mechanisms could be translated into an equivalent fracture energy heterogeneities, this work provides clues to optimize the disorder-induced toughening in a broader context.

Acknowledgements The author gratefully thanks Jean-Baptiste Leblond and Laurent Ponson for fruitful discussions, and the two anonymous reviewers whose comments improved the manuscript.

Conflict of interest

The author declares that he has no conflict of interest.

References

- Barés J, Hattali M, Dalmas D, Bonamy D (2014) Fluctuations of global energy release and crackling in nominally brittle heterogeneous fracture. *Physical Review Letters* 113(26):264301, DOI 10.1103/PhysRevLett.113.264301, URL <https://link.aps.org/doi/10.1103/PhysRevLett.113.264301>
- Barthelat F, Rabiei R (2011) Toughness amplification in natural composites. *Journal of the Mechanics and Physics of Solids* 59(4):829–840, DOI 10.1016/j.jmps.2011.01.001, URL <http://www.sciencedirect.com/science/article/pii/S0022509611000020>
- Bonamy D (2009) Intermittency and roughening in the failure of brittle heterogeneous materials. *Journal of Physics D: Applied Physics* 42(21):214014, DOI 10.1088/0022-3727/42/21/214014, URL <http://arxiv.org/abs/0907.3353>
- Bonamy D, Bouchaud E (2011) Failure of heterogeneous materials: A dynamic phase transition? *Physics Reports* 498(1):1–44, DOI 10.1016/j.physrep.2010.07.006, URL <http://www.sciencedirect.com/science/article/pii/S0370157310002115>
- Bouchaud E, Lapasset G, Plané J (1990) Fractal dimension of fractured surfaces: A universal value? *Europhysics Letters* 13(1):73–79, DOI 10.1209/0295-5075/13/1/013, URL <https://iopscience.iop.org/article/10.1209/0295-5075/13/1/013>
- Bower A, Ortiz M (1991) A three-dimensional analysis of crack trapping and bridging by tough particles. *Journal of the Mechanics and Physics of Solids* 39(6):815–858, DOI 10.1016/0022-5096(91)90026-K, URL <http://www.sciencedirect.com/science/article/pii/002250969190026K>
- Brach S, Hossain MZ, Bourdin B, Bhattacharya K (2019) Anisotropy of the effective toughness of layered media. *Journal of the Mechanics and Physics of Solids* 131:96–111, DOI 10.1016/j.jmps.2019.06.021, URL <http://www.sciencedirect.com/science/article/pii/S0022509619303333>
- Bueckner H (1970) Novel principle for the computation of stress intensity factors. *Zeitschrift fuer Angewandte Mathematik & Mechanik* 50(9), URL <https://trid.trb.org/view/3976>
- Chandler M, Meredith P, Brantut N, Crawford B (2016) Fracture toughness anisotropy in shale. *Journal of Geophysical Research: Solid Earth* 121(3):1706–1729, DOI 10.1002/2015JB012756, URL <https://agupubs.onlinelibrary.wiley.com/doi/abs/10.1002/2015JB012756>
- Chopin J, Prevost A, Boudaoud A, Adda-Bedia M (2011) Crack front dynamics across a single heterogeneity. *Physical Review Letters* 107(14):144301, DOI 10.1103/PhysRevLett.107.144301, URL <https://link.aps.org/doi/10.1103/PhysRevLett.107.144301>
- Chopin J, Bhaskar A, Jog A, Ponson L (2018) Depinning dynamics of crack fronts. *Physical Review Letters* 121(23):235501, DOI 10.1103/PhysRevLett.121.235501, URL <https://link.aps.org/doi/10.1103/PhysRevLett.121.235501>
- Dalmas D, Barthel E, Vandembroucq D (2009) Crack front pinning by design in planar heterogeneous interfaces. *Journal of the Mechanics and Physics of Solids* 57(3):446–457, DOI 10.1016/j.jmps.2008.11.012, URL <http://www.sciencedirect.com/science/article/pii/S002250960800210X>
- Delaplace A, Schmittbuhl J, Maloy K (1999) High resolution description of a crack front in a heterogeneous plexiglas block. *Physical Review E* 60(2):1337–1343, DOI 10.1103/PhysRevE.60.1337, URL <https://link.aps.org/doi/10.1103/PhysRevE.60.1337>
- Démary V, Lecomte V, Rosso A (2014a) Effect of disorder geometry on the critical force in disordered elastic systems. *Journal of Statistical Mechanics: Theory and Experiment* 2014(3):P03009, DOI 10.1088/1742-5468/2014/03/P03009, URL <http://arxiv.org/abs/1312.0468>
- Démary V, Rosso A, Ponson L (2014b) From microstructural features to effective toughness in disordered brittle solids. *EPL (Europhysics Letters)* 105(3):34003, DOI 10.1209/0295-5075/105/3/34003, URL <http://stacks.iop.org/0295-5075/105/i=3/a=34003>
- Dimas L, Bratzel G, Eylon I, Buehler M (2013) Tough composites inspired by mineralized natural materials: Computation, 3d printing, and testing. *Advanced Functional Materials* 23(36):4629–4638, DOI 10.1002/adfm.201300215, URL <https://onlinelibrary.wiley.com/doi/full/10.1002/adfm.201300215>
- Evans AG, Faber KT (1981) Toughening of ceramics by circumferential microcracking. *Journal of the American Ceramic Society* 64(7):394–398, DOI 10.1111/j.1151-2916.1981.tb09877.x, URL <https://ceramics.onlinelibrary.wiley.com/doi/abs/10.1111/j.1151-2916.1981.tb09877.x>
- Faber KT, Evans AG (1983) Crack deflection processes - i. theory. *Acta Metallurgica* 31(4):565–576, DOI 10.1016/0001-6160(83)90046-9, URL <http://www.sciencedirect.com/science/article/pii/0001616083900469>
- Gao H, Rice J (1989) A first-order perturbation analysis of crack trapping by arrays of obstacles. *Journal of Applied Mechanics* 56(4):828–836, DOI 10.1115/1.3176178, URL <http://dx.doi.org/10.1115/1.3176178>
- Griffith A (1921) The phenomena of rupture and flow in solids. *Phil Trans R Soc Lond A* 221, DOI 10.1098/rsta.1921.0006, URL <http://rsta.royalsocietypublishing.org/content/221/582-593/163>
- He M, Hutchinson J (1989) Crack deflection at an interface between dissimilar elastic materials. *International Journal of Solids and Structures* 25(9):1053–1067, DOI 10.1016/0020-7683(89)90021-8, URL <http://www.sciencedirect.com/science/article/pii/0020768389900218>
- Hossain MZ, Hsueh C, Bourdin B, Bhattacharya K (2014) Effective toughness of heterogeneous media. *Journal of the Mechanics and Physics of Solids* 71:15–32, DOI 10.1016/j.jmps.2014.06.002, URL <http://www.sciencedirect.com/science/article/pii/S0022509614001215>
- Hsueh C, Bhattacharya K (2018) Optimizing microstructure for toughness: the model problem of peeling. *Structural and Multidisciplinary Optimization* 58(3):1067–1080, DOI 10.1007/s00158-018-1952-0, URL <https://doi.org/10.1007/s00158-018-1952-0>
- Irwin GR (1957) Analysis of stresses and strains near the end of a crack transversing a plate. *Trans ASME, Ser E, J Appl Mech* 24:361–364, URL <https://ci.nii.ac.jp/naid/10016697098/>
- Jumel J, Shanahan MER (2008-09-22) Crack front curvature in the wedge test. *The Journal of Adhesion* 84(9):788–804, DOI 10.1080/00218460802352975, URL <https://doi.org/10.1080/00218460802352975>
- Kolvin I, Cohen G, Fineberg J (2015) Crack front dynamics: the interplay of singular geometry and crack instabilities. *Physical Review Letters* 114(17):175501, DOI 10.1103/PhysRevLett.114.175501
- Lapusta N, Rice JR (2003) Nucleation and early seismic propagation of small and large events in a crustal earthquake model. *Journal of Geophysical Research: Solid Earth* 108, DOI 10.1029/2001JB000793, URL <https://agupubs.onlinelibrary.wiley.com/doi/abs/10.1029/2001JB000793>
- Larkin A, Ovechinnikov Y (1979) Pinning in type II superconductors. *Journal of Low Temperature Physics* 34(3):409–428, DOI 10.1007/BF00117160, URL <https://doi.org/10.1007/BF00117160>
- Lebihain M (2019) Large-scale crack propagation in heterogeneous materials : an insight into the homogenization of brittle fracture properties. PhD thesis, Sorbonne Université
- Lebihain M, Leblond JB, Ponson L (2020) Effective toughness of periodic heterogeneous materials: the effect of out-of-plane excursions of cracks. *Journal of the Mechanics and Physics of Solids* 137:103876, DOI 10.1016/j.jmps.2020.103876, URL <http://www.sciencedirect.com/science/article/pii/S0022509619308464>
- Lebihain M, Ponson L, Kondo D, Leblond J (2021) Effective toughness of disordered brittle solids: a homogenization framework. accepted in the *Journal of the Mechanics and Physics of Solids*

- Legrand L, Patinet S, Leblond J, Frelat J, Lazarus V, Vandembroucq D (2011) Coplanar perturbation of a crack lying on the mid-plane of a plate. *International Journal of Fracture* 170(1):67–82, DOI 10.1007/s10704-011-9603-0, URL <https://doi.org/10.1007/s10704-011-9603-0>
- Leguillon D, Tariolle S, Martin E, Chartier T, Besson JL (2006) Prediction of crack deflection in porous/dense ceramic laminates. *Journal of the European Ceramic Society* 26(3):343–349, DOI 10.1016/j.jeurceramsoc.2004.11.003, URL <http://www.sciencedirect.com/science/article/pii/S0955221904005230>
- Lei M, Hamel CM, Yuan C, Lu H, Qi HJ (2018) 3d printed two-dimensional periodic structures with tailored in-plane dynamic responses and fracture behaviors. *Composites Science and Technology* 159:189–198, DOI 10.1016/j.compscitech.2018.02.024, URL <http://www.sciencedirect.com/science/article/pii/S0266353817325228>
- Malik I, Barthelat F (2016) Toughening of thin ceramic plates using bioinspired surface patterns. *International Journal of Solids and Structures* 97-98:389–399, DOI 10.1016/j.ijsolstr.2016.07.010, URL <http://www.sciencedirect.com/science/article/pii/S0020768316301640>
- Malik I, Barthelat F (2018) Bioinspired sutured materials for strength and toughness: Pullout mechanisms and geometric enrichments. *International Journal of Solids and Structures* 138:118–133, DOI 10.1016/j.ijsolstr.2018.01.004, URL <http://www.sciencedirect.com/science/article/pii/S0020768318300052>
- Máley KJ, Santucci S, Schmittbuhl J, Toussaint R (2006) Local waiting time fluctuations along a randomly pinned crack front. *Physical Review Letters* 96(4):045501, DOI 10.1103/PhysRevLett.96.045501, URL <https://link.aps.org/doi/10.1103/PhysRevLett.96.045501>
- Merta I, Tschegg EK (2013) Fracture energy of natural fibre reinforced concrete. *Construction and Building Materials* 40:991–997, DOI 10.1016/j.conbuildmat.2012.11.060, URL <http://www.sciencedirect.com/science/article/pii/S09550061812008963>
- Milton GW (2002) *The theory of composites*. Cambridge University Press, URL <http://dl.merc.ac.ir/handle/Hannan/3193>
- Ortiz M (1987) A continuum theory of crack shielding in ceramics. *Journal of Applied Mechanics* 54(1):54–58, DOI 10.1115/1.3172994, URL <http://dx.doi.org/10.1115/1.3172994>
- Patinet S, Alzate L, Barthel E, Dalmas D, Vandembroucq D, Lazarus V (2013a) Finite size effects on crack front pinning at heterogeneous planar interfaces: Experimental, finite elements and perturbation approaches. *Journal of the Mechanics and Physics of Solids* 61(2):311–324, DOI 10.1016/j.jmps.2012.10.012, URL <http://www.sciencedirect.com/science/article/pii/S0022509612002335>
- Patinet S, Vandembroucq D, Roux S (2013b) Quantitative prediction of effective toughness at random heterogeneous interfaces. *Physical Review Letters* 110(16):165507, DOI 10.1103/PhysRevLett.110.165507, URL <https://link.aps.org/doi/10.1103/PhysRevLett.110.165507>
- Ponson L (2009) Depinning transition in the failure of inhomogeneous brittle materials. *Physical Review Letters* 103(5):055501, DOI 10.1103/PhysRevLett.103.055501, URL <https://link.aps.org/doi/10.1103/PhysRevLett.103.055501>
- Ponson L, Bonamy D (2010) Crack propagation in brittle heterogeneous solids: Material disorder and crack dynamics. *International Journal of Fracture* 162(1):21–31, DOI 10.1007/s10704-010-9481-x, URL <https://doi.org/10.1007/s10704-010-9481-x>
- Ponson L, Pindra N (2017) Crack propagation through disordered materials as a depinning transition: A critical test of the theory. *Physical Review E* 95(5):053004, DOI 10.1103/PhysRevE.95.053004, URL <https://link.aps.org/doi/10.1103/PhysRevE.95.053004>
- Ponson L, Auradou H, Vié P, Hulin J (2006) Low self-affine exponents of fractured glass ceramics surfaces. *Physical Review Letters* 97(12):125501, DOI 10.1103/PhysRevLett.97.125501, URL <https://link.aps.org/doi/10.1103/PhysRevLett.97.125501>
- Ponte-Castañeda P, Suquet P (1997) Nonlinear composites. In: van der Giessen E, Wu TY (eds) *Advances in Applied Mechanics*, vol 34, Elsevier, pp 171–302, DOI 10.1016/S0065-2156(08)70321-1, URL <http://www.sciencedirect.com/science/article/pii/S0065215608703211>
- Rice J (1985) First-order variation in elastic fields due to variation in location of a planar crack front. *Journal of Applied Mechanics* 52(3):571–579, DOI 10.1115/1.3169103, URL <http://dx.doi.org/10.1115/1.3169103>
- Roux S, Hild F (2008) Self-consistent scheme for toughness homogenization. *International Journal of Fracture* 154(1):159–166, DOI 10.1007/s10704-008-9271-x, URL <https://doi.org/10.1007/s10704-008-9271-x>
- Roux S, Vandembroucq D, Hild F (2003) Effective toughness of heterogeneous brittle materials. *European Journal of Mechanics - A/Solids* 22(5):743–749, DOI 10.1016/S0997-7538(03)00078-0, URL <http://www.sciencedirect.com/science/article/pii/S0997753803000780>
- Vasoya M, Lazarus V, Ponson L (2016) Bridging micro to macroscale fracture properties in highly heterogeneous brittle solids: weak pinning versus fingering. *Journal of the Mechanics and Physics of Solids* 95:755–773, DOI 10.1016/j.jmps.2016.04.022, URL <http://www.sciencedirect.com/science/article/pii/S0022509615303604>
- Wang N, Xia S (2017) Cohesive fracture of elastically heterogeneous materials: An integrative modeling and experimental study. *Journal of the Mechanics and Physics of Solids* 98:87–105, DOI 10.1016/j.jmps.2016.09.004, URL <http://www.sciencedirect.com/science/article/pii/S0022509616303313>
- Widom B (1966) Random sequential addition of hard spheres to a volume. *The Journal of Chemical Physics* 44(10):3888–3894, DOI 10.1063/1.1726548, URL <https://aip.scitation.org/doi/abs/10.1063/1.1726548>
- Xia SM, Ponson L, Ravichandran G, Bhattacharya K (2013) Adhesion of heterogeneous thin films - i: Elastic heterogeneity. *Journal of the Mechanics and Physics of Solids* 61(3):838–851, DOI 10.1016/j.jmps.2012.10.014, URL <http://www.sciencedirect.com/science/article/pii/S0022509612002359>
- Xia SM, Ponson L, Ravichandran G, Bhattacharya K (2015) Adhesion of heterogeneous thin films - ii: Adhesive heterogeneity. *Journal of the Mechanics and Physics of Solids* 83:88–103, DOI 10.1016/j.jmps.2015.06.010, URL <http://www.sciencedirect.com/science/article/pii/S0022509615001593>